

# Configuration entropy and stability of bottomonium radial excitations in a plasma with magnetic fields

Nelson R. F. Braga<sup>\*</sup> and Yan F. Ferreira<sup>†</sup>

*Instituto de Física, Universidade Federal do Rio de Janeiro,  
Caixa Postal 68528, RJ 21941-972 – Brazil*

Luiz F. Ferreira<sup>‡</sup>

*CCNH, Universidade Federal do ABC – UFABC, 09210-580, Santo André – Brazil.*

## Abstract

Heavy vector mesons produced in a heavy ion collision are important sources of information about the quark gluon plasma (QGP). For instance, the fraction of bottomonium states observed in a such a collision is altered by the dissociation effect caused by the plasma. So, it is very important to understand how the properties of the plasma, like temperature, density and the presence of background magnetic fields, affect the dissociation of bottomonium in the thermal medium. AdS/QCD holographic models provide a tool for investigating the properties of heavy mesons inside a thermal medium. The meson states are represented by quasinormal modes in a black hole geometry. In this work we calculate the quasinormal modes and the associated complex frequencies for the four lowest levels of radial excitation of bottomonium inside a plasma with a magnetic field background. We also calculate the differential configuration entropy (DCE) for all these states and investigate how the dissociation effect produced by the magnetic field is translated into a dependence of the DCE on the field. An interesting result obtained in this study is that the DCE increases with the radial excitation level. Also, a non trivial finding of this work is that the energy density associated with the bottomonium quasinormal modes present a singularity near the black hole horizon. However, as we show here, it is possible to separate the singular factor and define a square integrable quantity that provides the DCE for the bottomonium states.

Keywords: Configuration Entropy, Quasinormal Modes, Quark Gluon Plasma, Quarkonium

---

<sup>\*</sup> [braga@if.ufrj.br](mailto:braga@if.ufrj.br)

<sup>†</sup> [yancarloff@pos.if.ufrj.br](mailto:yancarloff@pos.if.ufrj.br)

<sup>‡</sup> [luiz.faulhaber@ufabc.edu.br](mailto:luiz.faulhaber@ufabc.edu.br)

## I. INTRODUCTION

One of the most interesting challenges faced by physicists in the present days is to understand the properties of the quark gluon plasma (QGP). This state of matter, in which quarks and gluons interact strongly but are not confined into hadrons, is formed in heavy ion collisions. For reviews about the QGP, see for example [1–4]. The QGP lives for a very short time and the available information about it comes from the particles reaching the detectors after hadronization. Among those particles, bottomonium vector mesons, composed of a bottom anti-bottom quark pair are particularly important. These particles are created in the collision and then partially dissociate in the medium when the QGP is formed. The fraction of bottomonium final states observed in a heavy ion collision depends on how strong is the dissociation effect caused by the plasma. On the other hand, thermal dissociation depends on the properties of the plasma, such as: temperature, density and the presence of magnetic fields. That is why bottomonium can serve as an important probe of QGP properties.

The possibility of dissociation in the medium corresponds to a form of instability of bottomonium states. A very interesting tool to study stability of physical systems is the configuration entropy (CE). In recent years many examples appeared in the literature, involving various kinds of physical systems, where an increase in the configuration entropy (CE) is associated with an increase in the instability of the system, see for example [5–33]. In this work we use a holographic AdS/QCD model in order to represent bottomonium states in a plasma. We calculate the quasinormal modes, the associated complex frequencies and the corresponding CE for four different levels of radial excitation of bottomonium quasistates inside a plasma with a magnetic field background. Then we investigate how the instability, corresponding in this case to the dissociation in the thermal medium, is translated into a dependence of the configuration entropy on the field.

The CE is a continuous version of the information entropy introduced by Shannon: [34]

$$S_{\text{Shannon}} = - \sum_n p_n \ln p_n. \quad (1)$$

This quantity represents the amount of information contained in a variable  $x$  that can assume discrete values  $x_n$ , each of them with a probability  $p_n$ . Inspired by this definition, one

introduces the configuration entropy [7] in an analogous way, but for continuous variables:

$$S = - \int d^d \vec{k} \, \epsilon(\vec{k}) \ln \epsilon(\vec{k}), \quad (2)$$

where

$$\epsilon(\vec{k}) = \frac{|\tilde{R}(\vec{k})|^2}{\text{Max}(|\tilde{R}(\vec{k})|^2)}, \quad (3)$$

is called the modal fraction. It is defined using the momentum space Fourier transform of a normalizable (square integrable) function in coordinate space  $R(\vec{r})$ :

$$\tilde{R}(\vec{k}) = \int d^d \vec{r} \, R(\vec{r}) e^{-i\vec{k} \cdot \vec{r}}. \quad (4)$$

The energy density  $\rho(\vec{r})$  of the physical system is usually taken as the normalizable function  $R(\vec{r})$  which defines the modal fraction. One finds in the literature an alternative definition for the modal fraction, where in eq. (3) one uses the normalization integral of the square of  $\tilde{R}(\vec{k})$  in the denominator, instead of the maximum value. The definition that we use, that provides a positive-definite  $S$ , is in general called differential configuration entropy (DCE), so we will use this notation from this point on.

In reference [35], the authors used holography to study the dissociation of the ground state of charmonium in a plasma as function of the magnetic field  $B$  and calculated the corresponding configuration entropy. Here we consider bottomonium, that undergoes dissociation at higher temperatures, and study the dissociation of the different radial excitation levels, not only the ground state. This way, we will be able to analyze the dependence of the configuration entropy on the excitation level, that was not analyzed in this previous work. The lowest radial excitations of bottomonium survive the deconfinement transition and therefore are also important probes of the plasma properties.

This article is organized this way: in section II we review the holographic AdS/QCD bottom-up model that describes bottomonium in a plasma. In section III we obtain the quasinormal modes as functions of the magnetic field  $B$ . In section IV we use the field that represents the quasiparticles with corresponding quasinormal frequency to calculate the energy density of the system. Then, in section V, we use the results obtained in order to find the configuration entropy of the system. Finally, in section VI, we present a discussion about the results obtained.

## II. HOLOGRAPHIC DESCRIPTION OF BOTTOMONIUM IN A PLASMA WITH MAGNETIC FIELDS

The study of the kind of holographic model for heavy vector mesons that we will consider started in Refs. [36–38]. Then an improved version, that we will use here, was developed in Refs. [39–42]. This model provides good estimates not only for the quarkonium masses, but also for the decay constants. This is important since we are concerned in the study of bottomonium in the plasma. The decay constants are related to the heights of the peaks of the spectral functions. So that, it is crucial to have a nice fit for these quantities in order to describe quarkonium in a thermal medium [39]. For other approaches to the holographic description of bottomonium see, for example [43, 44].

Vector mesons are represented by a 5-dimensional dual vector field  $V_m$  with an action integral of the form<sup>1</sup>

$$I = -\frac{1}{4g_5^2} \int d^4x dz \sqrt{-g} \mathcal{L}, \quad (5)$$

with the Lagrangian density  $\mathcal{L} = e^{-\phi(z)} g^{mp} g^{nq} F_{mn}^* F_{pq}$ , where  $F_{mn} = \nabla_m V_n - \nabla_n V_m = \partial_m V_n - \partial_n V_m$ . We take the magnetic field in the  $x_3$  direction and use the metric [45]

$$ds^2 = \frac{R^2}{z^2} \left\{ -f(z) dt^2 + d(z) \left[ (dx^1)^2 + (dx^2)^2 \right] + h(z) (dx^3)^2 + \frac{1}{f(z)} dz^2 \right\}, \quad (6)$$

where<sup>2</sup>

$$f(z) = 1 - \frac{z^4}{z_h^4} + \frac{2}{3} \frac{e^2 B^2}{1.6^2} z^4 \ln \frac{z}{z_h}, \quad (7)$$

$$h(z) = 1 + \frac{8}{3} \frac{e^2 B^2}{1.6^2} z_h^4 \int_0^{z/z_h} \frac{y^3 \ln y}{1 - y^4} dy, \quad (8)$$

$$d(z) = 1 - \frac{4}{3} \frac{e^2 B^2}{1.6^2} z_h^4 \int_0^{z/z_h} \frac{y^3 \ln y}{1 - y^4} dy, \quad (9)$$

$R$  is the AdS radius and  $z_h$  is the horizon position. The plasma temperature is given by [46, 47]

$$T = \frac{|f'(z_h)|}{4\pi} = \frac{1}{4\pi} \left| \frac{4}{z_h} - \frac{2}{3} \frac{e^2 B^2}{1.6^2} \right|. \quad (10)$$

---

<sup>1</sup> Note that we are not studying the effect the magnetic field makes over the bottomonium itself, but over the background plasma. As consequence of it, the metric we use depends on  $B$  and the Lagrangian does not.

<sup>2</sup> One can find a primitive of  $(y^3 \ln y)/(1 - y^4)$  in terms of the polylogarithm function.

In the absence of the plasma ( $z_h \rightarrow \infty$ ) and of magnetic field ( $B \rightarrow 0$ ), that means, in the vacuum, the space is just a five dimensional anti-de Sitter one. The background field  $\phi(z)$  used is

$$\phi(z) = \kappa^2 z^2 + Mz + \tanh\left(\frac{1}{Mz} - \frac{\kappa}{\sqrt{\Gamma}}\right). \quad (11)$$

We take the masses and decay constants of bottomonium in the vacuum from the particle data group table[48] and the parameters that best fit them are  $\kappa_b = 2.45 \text{ GeV}$ ,  $\sqrt{\Gamma_b} = 1.55 \text{ GeV}$  and  $M_b = 6.2 \text{ GeV}$ .

We now choose a Fourier component of the field,  $V_m(t, \mathbf{x}, z) = \eta_m v(\omega, \mathbf{q}, z) e^{+i\eta_{\mu\nu} q^\mu x^\nu}$ , with polarization  $\eta_m$ . We choose the gauge  $V_z = 0$  and consider the vector meson at rest, so that  $\mathbf{q} = \mathbf{0}$ . This gives  $V_\mu(t, \mathbf{x}, z) = V_\mu(t, z) = \eta_\mu v(\omega, z) e^{-i\omega t}$ .

For transverse polarizations,  $\eta_\mu = (0, 1, 0, 0)$  and  $\eta_\mu = (0, 0, 1, 0)$ , we have

$$\frac{\omega^2}{f(z)^2} v(z) + \left(-\frac{1}{z} + \frac{f'(z)}{f(z)} + \frac{h'(z)}{2h(z)} - \phi'(z)\right) v'(z) + v''(z) = 0. \quad (12)$$

where the prime stands for the derivative with respect to  $z$  and, for simplicity, we use the notation  $v(z)$  for  $v(\omega, z)$ , omitting the dependency on  $\omega$ . For longitudinal polarization,  $\eta_\mu = (0, 0, 0, 1)$ , we have

$$\frac{\omega^2}{f(z)^2} v(z) + \left(-\frac{1}{z} + \frac{f'(z)}{f(z)} + \frac{d'(z)}{d(z)} - \frac{h'(z)}{2h(z)} - \phi'(z)\right) v'(z) + v''(z) = 0. \quad (13)$$

The solutions of equations (12) and (13), with appropriate boundary conditions, will provide the quasinormal modes.

### III. QUASINORMAL MODES

Quasinormal models (QNM) are field solutions, with complex frequencies, that satisfy incoming wave condition on the horizon and represent the meson quasistates. In order to find the QNMs one needs to analyze the behavior of the field near the horizon. One can expand the coefficients of  $v(z)$ ,  $v'(z)$  and  $v''(z)$  in (12) and (13) in powers of  $(z - z_h)$  and keep only the dominant terms. This gives, for longitudinal and transversal polarizations

$$\frac{\omega^2}{f'(z_h)^2 (z - z_h)^2} v_{\text{hor}}(z) + \frac{1}{z - z_h} v'_{\text{hor}}(z) + v''_{\text{hor}}(z) = 0, \quad (14)$$

where we used  $f(z_h) = 0$ . In terms of the temperature (10), we can write (14) as

$$\frac{\omega^2}{(4\pi T)^2} v_{\text{hor}}(z) + (z - z_h) v'_{\text{hor}}(z) + (z - z_h)^2 v''_{\text{hor}}(z) = 0, \quad (15)$$

whose solutions are

$$\left(1 - \frac{z}{z_h}\right)^{+i\omega/4\pi T} \quad \text{and} \quad \left(1 - \frac{z}{z_h}\right)^{-i\omega/4\pi T}. \quad (16)$$

The second solution, with negative exponent, corresponds to an infalling wave at the horizon, while the first solution, with positive exponent to an outgoing wave. This becomes clear if one change to the Regge-Wheeler tortoise coordinate [49]. The quasinormal complex frequencies are found by imposing the field to satisfy the condition of being an infalling wave at the horizon, and the Dirichlet condition at the boundary  $v(0) = 0$  [50, 51].

We find the quasinormal field  $v(z)$  in terms of  $\omega$  by solving the complete equations of motion (12) and (13) numerically with the conditions  $v(z_0) = v_{\text{hor},p}(z_0)$  and  $v'(z_0) = v'_{\text{hor},p}(z_0)$ , where  $z_0 = z_h - \epsilon$ , with  $\epsilon$  small, and  $v_{\text{hor},p}$  is taken in the form

$$v_{\text{hor},p}(z) = \left(1 - \frac{z}{z_h}\right)^{-i\omega/4\pi T} \sum_{n=0}^p a_n \left(1 - \frac{z}{z_h}\right)^n, \quad (17)$$

which is the infalling horizon solution  $v_{\text{hor}}$  times a polynomial perturbation introduced in order to calculate the field at  $z_0 = z_h - \epsilon$ . The first coefficient of the polynomial perturbation is  $a_0 = 1$  and the other coefficients  $a_n$  are determined by substituting (17) into the equation of motion (12), for longitudinal polarization, or (13), for transverse polarization. This is how we impose the infalling wave condition at the horizon in the numerical calculation.

It is important to note that due to the highly oscillatory behavior of the factor  $(1 - z/z_h)^{-i\omega/4\pi T}$  near  $z = z_h$ ,  $\epsilon$  cannot be too small [50]. On the other hand, the larger is the value of  $\epsilon$ , the greater must be  $p$ , the order of the polynomial perturbation in (17). One has to consider this two factors in order to fix the value of  $\epsilon$ .

Following this procedure we build a parametric numerical solution of the equation of motion with parameter  $\omega$ . With this parametric numerical solution we impose the Dirichlet condition at the boundary by numerically solving the equation  $v(\omega, z=0) = 0$  for complex  $\omega$ . This determines the quasinormal frequency. The numeric solution of the equation of motion with the value of  $\omega$  obtained will then give the field  $v$  in the interval from 0 to  $z_0$ .

The results of quasinormal frequencies for transverse and longitudinal polarizations as function of the magnetic field  $B$  and for temperature fixed at  $T = 300 \text{ MeV}$  are shown in figures 1 and 2, respectively.

The real part of the quasinormal frequency is interpreted as the thermal mass of the quasiparticle and the imaginary part is related to the degree of dissociation. The larger the absolute value of the imaginary part, the stronger the dissociation.

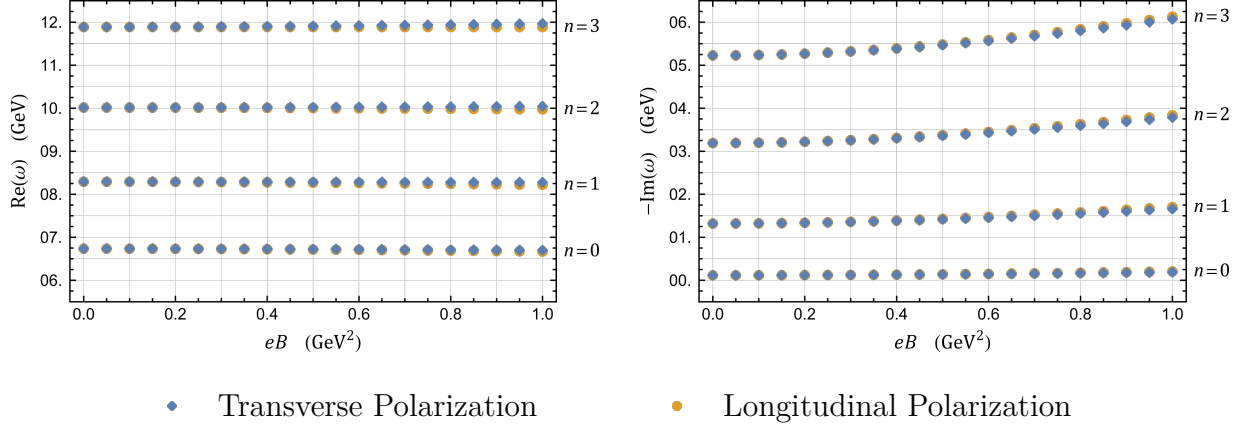


Figure 1. Quasinormal frequencies for transverse and longitudinal polarizations of the different excitation levels as function of the magnetic field  $B$  and for temperature fixed at  $T = 300$  MeV.

#### IV. ENERGY DENSITY

The energy density  $\rho(z)$  of our system is the  $T_{00}$  component of the energy-momentum tensor which, as in general relativity, can be calculated from

$$T_{mn}(z) = \frac{2}{\sqrt{-g}} \left[ \frac{\partial(\sqrt{-g} \mathcal{L})}{\partial g^{mn}} - \partial_p \frac{\partial(\sqrt{-g} \mathcal{L})}{\partial(\partial_p g^{mn})} \right]. \quad (18)$$

For transverse polarization fields, the energy density becomes

$$\rho(z) = -\frac{e^{2\text{Im}(\omega)t}}{2g_5^2 R^2} \frac{z^2 e^{-\phi(z)}}{d(z)} \left( |\omega v(z)|^2 + f(z)^2 |v'(z)|^2 \right) \quad (19)$$

and for longitudinal polarization fields, it becomes

$$\rho(z) = -\frac{e^{2\text{Im}(\omega)t}}{2g_5^2 R^2} \frac{z^2 e^{-\phi(z)}}{h(z)} \left( |\omega v(z)|^2 + f(z)^2 |v'(z)|^2 \right). \quad (20)$$

The solutions of the transverse and longitudinal equations of motion can be written in the form

$$v(z) = \left( 1 - \frac{z}{z_h} \right)^{-i\omega/4\pi T} \sum_{n=0}^{\infty} a_n \left( 1 - \frac{z}{z_h} \right)^n, \quad (21)$$

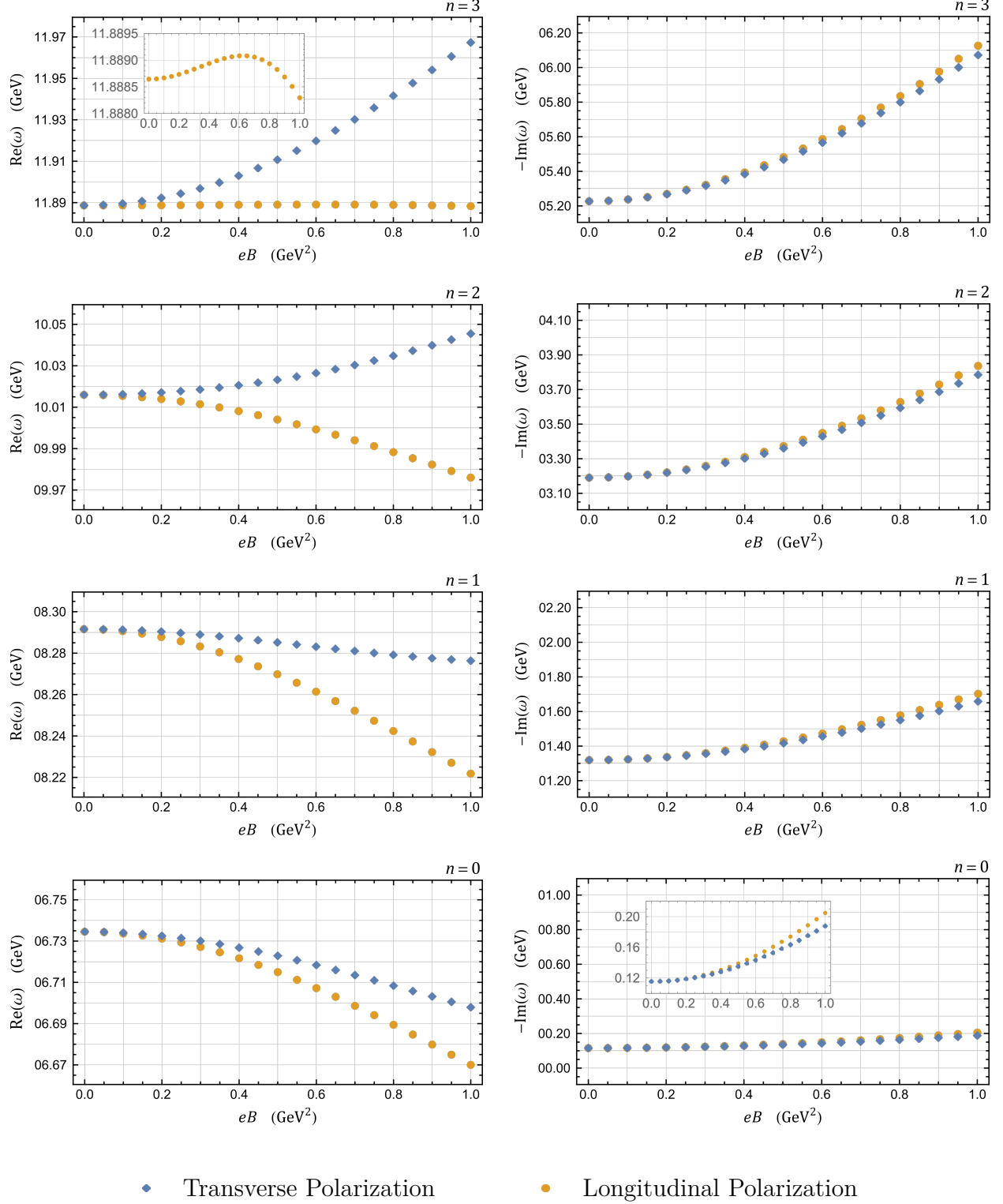


Figure 2. Quasinormal frequencies for transverse and longitudinal polarizations of the different excitation levels as function of the magnetic field  $eB$  and for  $T = 300 \text{ MeV}$ . All the plots of the real part of  $\omega$  have the same scale in order to make it easier the comparison of the variations. The same holds for the plots of the imaginary part.



which is the limit for  $p \rightarrow \infty$  of equation (17). Again,  $a_0 = 1$  and the other  $a_n$  coefficients are determined recursively from the equation of motion and the numerical evaluation is actually performed with a finite number of terms that is determined by checking the convergence of the procedure.

It is possible to write  $\rho(z)$  in the form

$$\rho(z) = \left(1 - \frac{z}{z_h}\right)^{\text{Im}(\omega)/2\pi T} \sum_{n=0}^{\infty} b_n \left(1 - \frac{z}{z_h}\right)^n, \quad (22)$$

where the series is obtained by substituting the field given by (21), taking the Taylor series of the factors that accompany  $|v|^2$  and  $|v'|^2$ , multiplying the series accordingly to (19) or (20) and ordering the terms.

If we now try to compute the integral  $\int_0^{z_h} \rho(z) dz$  we will have a problem: due to the singular<sup>3</sup> factor  $(1 - z/z_h)^{\text{Im}(\omega)/2\pi T}$ , the integral diverges for any value of  $\text{Im}(\omega)$  whose absolute value is greater than  $2\pi T$ . In fact,  $(1 - z/z_h)^{\text{Im}(\omega)/2\pi T}$  behaves near  $z = z_h$  as  $x^{\text{Im}(\omega)/2\pi T}$  behaves near  $x = 0$  and  $\int_0^b x^{-a} dx$  diverges for  $a \geq 1$  and for any  $b$ . The energy density is, therefore, a non-normalizable function if  $|\text{Im}(\omega)| \geq 2\pi T$  and it happens in the second excited states and above.<sup>4</sup> One can not use a non-normalizable function to define the modal fraction. So, we extract the factor  $(1 - z/z_h)^{\text{Im}(\omega)/2\pi T}$ , responsible for the divergence, keeping only the regular factor. This is achieved by simply introducing

$$R(z) = \left(1 - \frac{z}{z_h}\right)^{-\text{Im}(\omega)/2\pi T} \rho(z) = \sum_{n=0}^{\infty} b_n \left(1 - \frac{z}{z_h}\right)^n, \quad (23)$$

whose Fourier transform is

$$\tilde{R}(k) = \int_0^{z_h} R(z) e^{-ikz} dz. \quad (24)$$

Then we define the modal fraction as

$$\epsilon(k) = \frac{|\tilde{R}(k)|^2}{\text{Max}(|\tilde{R}(k)|^2)}. \quad (25)$$

The maximum value of  $|\tilde{R}(k)|^2$  is at  $k = 0$ .

An important detail of the numerical calculation that is worth noting is that, due to the highly oscillatory behavior of the factor  $(1 - z/z_h)^{-i\omega/4\pi T}$  near  $z = z_h$ , we do not evaluate the

<sup>3</sup> Remember that  $\text{Im}(\omega)$  is a negative value.

<sup>4</sup> See figure (2). There we can find that for  $n = 2$  and  $n = 3$ ,  $|\text{Im}(\omega)|$  is always bigger than  $2\pi \times 300 \text{ MeV} \simeq 1.88 \text{ GeV}$

field  $v$  in the region  $z_0 < z < z_h$ . However, we can evaluate  $R(z)$  directly in this region by using the series expansion in (23) and the fact that the coefficients  $b_n$  of the energy density can be written in terms of the coefficients  $a_n$  of the field.

## V. DIFFERENTIAL CONFIGURATION ENTROPY

Using the numerical solutions described in the last section, one obtains the modal fraction  $\epsilon(k)$  from eq. (25) and then finds the differential configuration entropy (DCE)

$$S = - \int_{-\infty}^{+\infty} \epsilon(k) \ln \epsilon(k) dk. \quad (26)$$

It is important to remark that the quasinormal mode solutions, and consequently the DCE, depend on  $T$  and  $B$ . We fixed the temperature at  $T = 300$  MeV that is a value of  $T$  in which the plasma is present but the bottomonium states are only partially dissociated. The result obtained for the DCE as function of  $eB$  is shown in figure 3, where we plot the four lowest radial modes  $n = 0, 1, 2, 3$  together in order to show the variation of the DCE with the excitation level. From this figure it is observed that the DCE increases with the excitation level. A result that is consistent with the fact that the higher order states are more unstable against dissociation in the thermal medium.

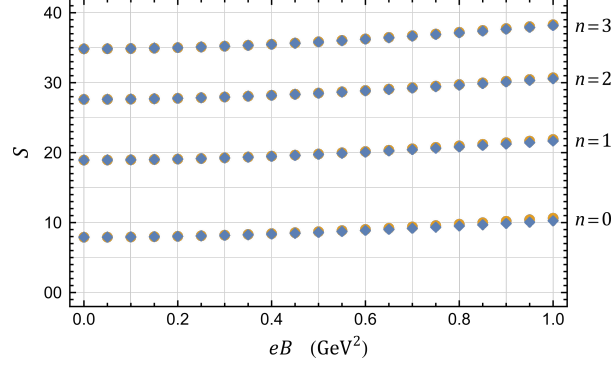
Then, in the four panels of figure 4, we show the DCE for each of the four lowest radial modes, with an expanded scale in order to make it possible to notice the variation with the magnetic field and the split between longitudinal and transverse modes. From this figure one notices that the DCE increases with the magnetic field, indicating an enhancement of the dissociation in the medium. This effect is slightly larger for the longitudinal polarization case.

Remarkably, the dependence of the DCE on the field  $eB$  is found to be of a simple form. The results obtained can be fitted by a polynomial of degree two in the magnetic field

$$S = c_0 + c_1(eB) + c_2(eB)^2, \quad (27)$$

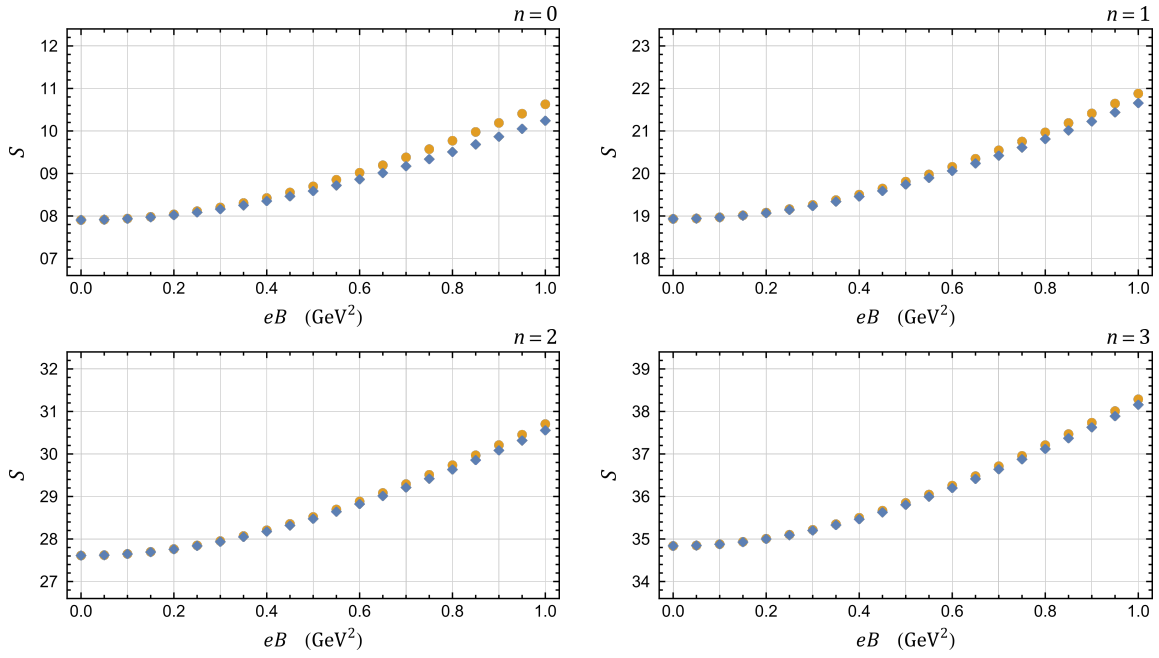
with values of the adjusted coefficient of determination,  $R_{\text{adj}}^2$  very close to one, indicating a very nice fit. We show the results of the fit on tables I and II.

As an illustration of the quadratic fit, we show in Figure 5 the actual values of the DCE, represented by points, and a line corresponding to the fit. We have taken the case of



• Transverse Polarization      • Longitudinal Polarization

Figure 3. Differential configuration entropy for transverse and longitudinal polarizations of the different excitation levels as a function of the magnetic field  $eB$  at  $T = 300$  MeV.



• Transverse Polarization      • Longitudinal Polarization

Figure 4. Differential configuration entropy for transverse and longitudinal polarizations of the  $n = 0, 1, 2, 3$  excitation levels as a function of the field  $eB$  for  $T = 300$  MeV. All the plots of the DCE have the same scale in order to make it easier the comparison of the variations.

transverse polarization and  $n = 0$  as an example. The plots for the other states are similar.

$n$	$c_0$	$c_1$ (GeV $^{-2}$ )	$c_2$ (GeV $^{-4}$ )	$R_{\text{adj}}^2$
1	$07.87 \pm 0.01$	$0.46 \pm 0.06$	$1.95 \pm 0.06$	0.9999942
2	$18.89 \pm 0.02$	$0.59 \pm 0.07$	$2.23 \pm 0.07$	0.9999981
3	$27.56 \pm 0.02$	$0.61 \pm 0.08$	$2.44 \pm 0.07$	0.9999991
4	$34.78 \pm 0.02$	$0.66 \pm 0.09$	$2.77 \pm 0.08$	0.9999992

Table I. Coefficients of the fit of the DCE for transverse polarization of the different excitation levels with the form given in eq. (27) for temperature fixed at  $T = 300$  MeV.

$n$	$c_0$	$c_1$ (GeV $^{-2}$ )	$c_2$ (GeV $^{-4}$ )	$R_{\text{adj}}^2$
1	$07.86 \pm 0.01$	$0.53 \pm 0.07$	$2.28 \pm 0.07$	0.9999925
2	$18.88 \pm 0.02$	$0.65 \pm 0.08$	$2.40 \pm 0.08$	0.9999978
3	$27.56 \pm 0.02$	$0.64 \pm 0.08$	$2.56 \pm 0.08$	0.9999990
4	$34.78 \pm 0.02$	$0.71 \pm 0.09$	$2.86 \pm 0.09$	0.9999992

Table II. Coefficients of the fit of the DCE for longitudinal polarization of the different excitation levels with the form given in eq. (27) for temperature fixed at  $T = 300$  MeV.

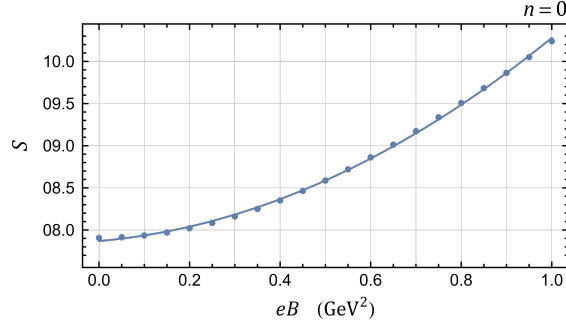


Figure 5. Quadratic fit of the differential configuration entropy of bottomonium field with transverse polarizations in the ground state as a function of the magnetic field  $eB$  for  $T = 300$  MeV.

## VI. CONCLUSIONS

We presented in this paper the results of the numerical computations of the quasinormal modes associated with the four lowest radial excitation levels of bottomonium in a plasma with a constant background magnetic field  $eB$ . Using these solutions we obtained the DCE for these states and analysed the dependence on the field. The result obtained shows that the DCE increases with the radial excitation level and also with the value of the field  $eB$ .

As discussed in the introduction, for many different systems it has been observed that the DCE works as an indicator of stability. The more stable the system is, the lower the value of the DCE. Therefore, our results are consistent with the fact that the higher excited states of bottomonium are subject to a stronger dissociation effect in the plasma, so that they are more unstable.

On the other hand, it is known from the calculation of spectral functions that the presence of magnetic fields enhances the dissociation effect of bottomonium in a plasma [42]. So that, increasing the  $eB$  field it is expected that the bottomonium quasistates become more unstable. This is consistent with our finding that the DCE increases with the magnetic field.

The same kind of behavior was inferred from the analysis of the imaginary part of the quasinormal frequencies  $\text{Im}(\omega)$ . As shown in figure 2,  $|\text{Im}(\omega)|$  increases with the value of the excitation level  $n$  and with the field  $eB$ . An increase in this quantity is associated with an enhancement in the dissociation in the medium and, thus, with instability. However, the increase in  $|\text{Im}(\omega)|$  with the field obtained here is stronger for the larger values of  $n$ . In contrast, for the DCE the effect of the variation with the magnetic field is approximately the same for all values of  $n$ . This fact can be seen as an indication that the DCE should not be taken as a quantitative measure of the dissociation. We mean: we confirmed for the bottomonium excited states in a magnetic field background that the higher is the DCE, the more unstable the system. However, we noticed that the rate of increase in the DCE should not be taken as a rate of increase in the degree of instability.

For some alternative interesting approaches to quarkonium in a thermal medium, see for example [52, 53].

**Acknowledgments:** N.R.F. B. is partially supported by CNPq - Conselho Nacional de Desenvolvimento Científico e Tecnológico grant 307641/2015-5 and both authors received support from Coordenação de Aperfeiçoamento de Pessoal de Nível Superior - Brasil (CAPES) - Finance Code 001.

- 
- [1] S. A. Bass, M. Gyulassy, H. Stoecker and W. Greiner, J. Phys. G **25**, R1 (1999) doi:10.1088/0954-3899/25/3/013 [hep-ph/9810281].
  - [2] S. Scherer *et al.*, Prog. Part. Nucl. Phys. **42**, 279 (1999). doi:10.1016/S0146-6410(99)00083-6

- [3] E. Shuryak, Prog. Part. Nucl. Phys. **62**, 48 (2009) doi:10.1016/j.ppnp.2008.09.001 [arXiv:0807.3033 [hep-ph]].
- [4] J. Casalderrey-Solana, H. Liu, D. Mateos, K. Rajagopal and U. A. Wiedemann, book:Gauge/String Duality, Hot QCD and Heavy Ion Collisions. Cambridge, UK: Cambridge University Press, 2014 doi:10.1017/CBO9781139136747 [arXiv:1101.0618 [hep-th]].
- [5] M. Gleiser and N. Stamatopoulos, Phys. Lett. B **713**, 304 (2012) [arXiv:1111.5597 [hep-th]].
- [6] M. Gleiser and N. Stamatopoulos, Phys. Rev. D **86**, 045004 (2012) [arXiv:1205.3061 [hep-th]].
- [7] M. Gleiser and D. Sowinski, Phys. Lett. B **727**, 272 (2013) [arXiv:1307.0530 [hep-th]].
- [8] A. E. Bernardini, N. R. F. Braga and R. da Rocha, Phys. Lett. B **765**, 81 (2017), [arXiv:1609.01258 [hep-th]].
- [9] N. R. F. Braga and R. da Rocha, Phys. Lett. B **776**, 78 (2018) [arXiv:1710.07383 [hep-th]].
- [10] N. R. F. Braga, L. F. Ferreira and R. Da Rocha, Phys. Lett. B **787**, 16 (2018) [arXiv:1808.10499 [hep-ph]].
- [11] L. F. Ferreira and R. Da Rocha, Phys. Rev. D **99**, no. 8, 086001 (2019) [arXiv:1902.04534 [hep-th]].
- [12] N. R. F. Braga, Phys. Lett. B **797**, 134919 (2019) doi:10.1016/j.physletb.2019.134919 [arXiv:1907.05756 [hep-th]].
- [13] R. A. C. Correa and R. da Rocha, Eur. Phys. J. C **75**, no. 11, 522 (2015) doi:10.1140/epjc/s10052-015-3735-8 [arXiv:1502.02283 [hep-th]].
- [14] N. R. F. Braga and R. da Rocha, Phys. Lett. B **767**, 386 (2017) [arXiv:1612.03289 [hep-th]].
- [15] G. Karapetyan, EPL **117**, no. 1, 18001 (2017) [arXiv:1612.09564 [hep-ph]].
- [16] G. Karapetyan, EPL **118** (2017) 38001 [arXiv:1705.10617 [hep-ph]].
- [17] G. Karapetyan, Phys. Lett. B **781** (2018) 201 [arXiv:1802.09105 [nucl-th]].
- [18] G. Karapetyan, Phys. Lett. B **786** (2018) 418 [arXiv:1807.04540 [nucl-th]].
- [19] C. O. Lee, Phys. Lett. B **790** (2019) 197 [arXiv:1812.00343 [gr-qc]].
- [20] D. Bazeia, D. C. Moreira and E. I. B. Rodrigues, J. Magn. Magn. Mater. **475** (2019) 734.
- [21] C. W. Ma and Y. G. Ma, Prog. Part. Nucl. Phys. **99**, 120 (2018) [arXiv:1801.02192 [nucl-th]].
- [22] Q. Zhao, B. Z. Mi and Y. Li, Int. J. Mod. Phys. B **33**, no. 12, 1950119 (2019).
- [23] L. F. Ferreira and R. da Rocha, Eur. Phys. J. C **80** (2020) no.5, 375 doi:10.1140/epjc/s10052-020-7978-7 [arXiv:1907.11809 [hep-th]].
- [24] G. Karapetyan, EPL **129**, no. 1, 18002 (2020) doi:10.1209/0295-5075/129/18002

- [arXiv:1912.10071 [hep-ph]].
- [25] N. R. F. Braga and R. da Mata, Phys. Rev. D **101**, no.10, 105016 (2020) doi:10.1103/PhysRevD.101.105016 [arXiv:2002.09413 [hep-th]].
  - [26] G. Karapetyan, [arXiv:2003.08994 [hep-ph]].
  - [27] L. F. Ferreira and R. da Rocha, Phys. Rev. D **101**, no.10, 106002 (2020) doi:10.1103/PhysRevD.101.106002 [arXiv:2004.04551 [hep-th]].
  - [28] A. Alves, A. G. Dias and R. da Silva, doi:10.1016/j.nuclphysb.2020.115137 [arXiv:2004.08407 [hep-ph]].
  - [29] D. Marinho Rodrigues and R. da Rocha, [arXiv:2006.00332 [hep-th]].
  - [30] M. Stephens, S. Vannah and M. Gleiser, Phys. Rev. D **102**, no.12, 123514 (2020) doi:10.1103/PhysRevD.102.123514 [arXiv:1905.07472 [astro-ph.CO]].
  - [31] D. Bazeia and E. I. B. Rodrigues, Phys. Lett. A **392**, 127170 (2021) doi:10.1016/j.physleta.2021.127170
  - [32] N. R. F. Braga and O. C. Junqueira, Phys. Lett. B **814**, 136082 (2021) doi:10.1016/j.physletb.2021.136082 [arXiv:2010.00714 [hep-th]].
  - [33] N. R. F. Braga and O. C. Junqueira, Phys. Lett. B **820** (2021), 136485 doi:10.1016/j.physletb.2021.136485 [arXiv:2105.12347 [hep-th]].
  - [34] C. E. Shannon, Bell Syst. Tech. J. **27**, 379-423 (1948)
  - [35] N. R. F. Braga and R. da Mata, Phys. Lett. B **811**, 135918 (2020) doi:10.1016/j.physletb.2020.135918 [arXiv:2008.10457 [hep-th]].
  - [36] N. R. F. Braga, M. A. Martin Contreras and S. Diles, Phys. Lett. B **763**, 203 (2016) [arXiv:1507.04708 [hep-th]].
  - [37] N. R. F. Braga, M. A. Martin Contreras and S. Diles, Eur. Phys. J. C **76**, no. 11, 598 (2016) [arXiv:1604.08296 [hep-ph]].
  - [38] N. R. F. Braga and L. F. Ferreira, Phys. Lett. B **773**, 313 (2017) [arXiv:1704.05038 [hep-ph]].
  - [39] N. R. F. Braga, L. F. Ferreira and A. Vega, Phys. Lett. B **774**, 476 (2017) [arXiv:1709.05326 [hep-ph]].
  - [40] N. R. F. Braga and L. F. Ferreira, Phys. Lett. B **783**, 186 (2018) [arXiv:1802.02084 [hep-ph]].
  - [41] N. R. F. Braga and L. F. Ferreira, JHEP **1901**, 082 (2019) doi:10.1007/JHEP01(2019)082 [arXiv:1810.11872 [hep-ph]].
  - [42] N. R. F. Braga and L. F. Ferreira, Phys. Lett. B **795**, 462-468 (2019)

- doi:10.1016/j.physletb.2019.06.050 [arXiv:1905.11309 [hep-ph]].
- [43] M. A. Martin Contreras, S. Diles and A. Vega, Phys. Rev. D **103**, no.8, 086008 (2021) doi:10.1103/PhysRevD.103.086008 [arXiv:2101.06212 [hep-ph]].
  - [44] R. Zöllner and B. Kämpfer, [arXiv:2109.05824 [hep-th]].
  - [45] D. Dudal, D. R. Granado and T. G. Mertens, Phys. Rev. D **93**, no. 12, 125004 (2016) doi:10.1103/PhysRevD.93.125004 [arXiv:1511.04042 [hep-th]].
  - [46] S. W. Hawking, Nature **248**, 30-31 (1974) doi:10.1038/248030a0
  - [47] S. W. Hawking, Commun. Math. Phys. **43**, 199-220 (1975) [erratum: Commun. Math. Phys. **46**, 206 (1976)] doi:10.1007/BF02345020
  - [48] P.A. Zyla *et al.* [Particle Data Group], PTEP **2020**, no.8, 083C01 (2020) doi:10.1093/ptep/ptaa104
  - [49] L. A. H. Mamani, A. S. Miranda, H. Boschi-Filho and N. R. F. Braga, JHEP **1403**, 058 (2014) doi:10.1007/JHEP03(2014)058 [arXiv:1312.3815 [hep-th]].
  - [50] M. Kaminski, K. Landsteiner, F. Pena-Benitez, J. Erdmenger, C. Greubel and P. Kerner, JHEP **1003**, 117 (2010) doi:10.1007/JHEP03(2010)117 [arXiv:0911.3544 [hep-th]].
  - [51] S. Janiszewski and M. Kaminski, Phys. Rev. D **93**, no. 2, 025006 (2016) [arXiv:1508.06993 [hep-th]].
  - [52] D. Dudal and T. G. Mertens, Phys. Rev. D **91**, 086002 (2015) doi:10.1103/PhysRevD.91.086002 [arXiv:1410.3297 [hep-th]].
  - [53] D. Dudal and T. G. Mertens, Phys. Rev. D **97**, no. 5, 054035 (2018) doi:10.1103/PhysRevD.97.054035 [arXiv:1802.02805 [hep-th]].